Entropic Tension in Crowded Membranes – Supplementary information

Martin Lindén,[1,*] Pierre Sens,[2,†] and Rob Phillips[1,2,‡]

[1] *California Institute of Technology, Pasadena, California 91125, U.S.A.*

[2] *Laboratoire de Physico-Chimie Théorique CNRS/UMR 7083 - ESPCI, 75231 Paris Cedex 05, France*

(Dated: January 20, 2011)

I. DIVERSITY IN MEMBRANE PROTEIN SIZE

As pointed out in the main body of the paper, membranes are a crowded conglomerate of lipids and their partner proteins. Simple estimates of the extent of this crowding can be based upon an "average" membrane protein with a generic disk shape and a fixed radius from one protein to the next. Of course, membrane proteins are much more heterogeneous than indicated by such a simple estimate. In this section, we count transmembrane helices to try to quantify the effect of protein size variation on crowding. Our estimate indicates that although there is a significant size variation, the effect on crowding is probably not very large.

The scaled particle theory described in the next section can capture some aspects of crowder heterogeneity, namely the distribution of protein size [1, 2]. In the simplest case of crowding by circular disks with different radii, the variation in protein size enters through the mean value and second moment of the disk radius R, and can be characterized (see Eq. (S9)) by the dimensionless parameter

$$\eta^2 = \frac{\langle R^2\rangle - \langle R\rangle^2}{\langle R^2\rangle} = \frac{\mathrm{Var}[R]}{\langle R^2\rangle}, \tag{S1}$$

where $\langle . \rangle$ denotes an average over all proteins. As a result, it is of interest to try and improve our understanding of the membrane census by explicitly examining the heterogeneity in membrane protein size.

Our starting point for this analysis is to categorize different membrane proteins by the number of transmembrane alpha helices (TMH) they have. Several bioinformatics tools can predict the number n_{TMH} of transmembrane helices of membrane protein sequences [3], and the results of such predictions are routinely reported in surveys of proteins or putative protein-coding DNA regions [4–6]. Figure S1 illustrates two transmembrane helix distributions, based on a synaptic vesicle model [5] and a proteomics study of the outer membrane of the Gram-negative bacterium *Acinetobacter baumannii* [4].

A simple estimate of η^2 is to approximate the protein footprint by a disk, whose area is proportional to the number of transmembrane helices. This leads to

$$\eta^2 \approx \eta^2_{\mathrm{TMH}} = \frac{\langle n_{\mathrm{TMH}}\rangle - \langle \sqrt{n_{\mathrm{TMH}}}\rangle^2}{\langle n_{\mathrm{TMH}}\rangle}. \tag{S2}$$

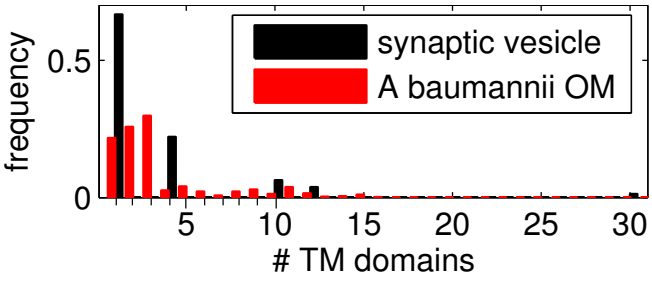

FIG. S1. Relative abundance of membrane proteins with different number of transmembrane (TM) helices, based on data for synaptic vesicles [5], and the outer membrane (OM) of the Gram-negative bacterium *A. baumannii* [4].

The synaptic vesicle study contains a list of membrane proteins in a 'typical' vesicle, estimated to account for almost 70% of the protein mass. We excluded proteins with no predicted transmembrane helices, and calculated

$$\langle n_{TMH}\rangle = 3.0, \quad \mathrm{Std}[n_{TMH}] = 4.3, \text{ and } \eta^2_{\mathrm{TMH}} = 0.25. \tag{S3}$$

The bacterial study reported several different estimates of relative abundance, which differ significantly in specific cases, but lead to similar overall distributions (not shown). We included proteins with predicted localization to the outer membrane, excluded proteins with no predicted transmembrane helices, and computed the average of the different abundance estimates. This gave the histogram in figure S1, as well as

$$\langle n_{TMH}\rangle = 3.5, \quad \mathrm{Std}[n_{TMH}] = 3.1, \text{ and } \eta^2_{\mathrm{TMH}} = 0.14. \tag{S4}$$

It is interesting to note the similarities in distributions in Fig. S1, both being dominated by proteins with a few TM helices, and spanning about one order of magnitude. However, there are several significant sources of uncertainty. For example, not all membrane proteins were detected, and we have neglected aggregation of protein subunits into larger complexes. Also, not all proteins have a near-circular areal footprint, as we assumed by using η^2_{TMH}.

As we will see below (Eq. (S9)), the variability enters the surface tension through the factor $1-\phi\eta^2$. With surface coverage ϕ on the order of 0.5, and η^2 on the order

* linden@caltech.edu
† pierre.sens@espci.fr
‡ phillips@pboc.caltech.edu

TABLE SI. List of symbols.

n_{TMH}	number of transmembrane (TM) helices	
β	inverse temperature scale	$\beta = 1/k_B T$
$\vec{n}$	copy number vector	$\vec{n} = (n_1, n_2, \ldots)$
n	total copy number	$n = \sum_j n_j$
$\vec{N}$	copy number vector for the crowders	$\vec{N} = (N_1, N_2, \ldots)$
N	total number of crowders	$N = \sum_{j \neq o,c} N_j$
A	area	
σ	surface tension (2D analog of negative pressure)	
c_A	areal number density	$c_A = n/A$
R_i	In-plane radius of species i. In particular, $i = o, c$ for the open and closed channel conformations respectively.	
F	Helmholtz free energy (constant area ensemble)	
G	Gibbs free energy (constant tension ensemble)	$G = F - \sigma A$
ΔC	circumference change of channel	$\Delta C = 2\pi(R_o - R_c)$
ΔA	area change of channel	$\Delta A = \pi(R_o^2 - R_c^2)$
$\langle R^m \rangle$	mth moment of the protein radius distribution	$\langle R^m \rangle = \frac{1}{n} \sum_j n_j R_j^m$
$\mathrm{Var}[R]$	radius variance	$\mathrm{Var}[R] = \langle R^2 \rangle - \langle R \rangle^2$
$\langle R_p^m \rangle$	mth moment of the crowder radius distribution	$\langle R_p^m \rangle = \frac{1}{N} \sum_{j \neq o,c} N_j R_j^m$
R_p	crowder radius, for the case of uniform crowder size	
ϕ	area fraction of disks or proteins	$\phi = c_A \pi \langle R^2 \rangle$
A_0	total area occupied by unstretched lipids	$A_0 = A(1 - \phi) = A - n\pi\langle R^2 \rangle$
η^2	relative protein radius variance	$\eta^2 = \mathrm{Var}[R]/\langle R^2 \rangle$
$A_{\vec{n}}$	unstretched equilibrium area in constant tension ensemble	$A_{\vec{n}} = A_0 + n\pi\langle R^2 \rangle$.

of 0.2, our tentative estimate based upon an unsatisfying dearth of data on the relative and absolute abundances of membrane proteins is that protein size variability does not constitutes a major correction to the crowding tension.

II. BASIC RESULTS OF SCALED PARTICLE THEORY

In this section, we restate some basic results of scaled-particle theory for use in our subsequent calculations. We will express the results in terms of area, temperature, and particle copy numbers, since this is what we will use as thermodynamic control variables, but also quote the results in terms of variables like concentration c_A and area fraction ϕ.

Scaled-particle theory has been generalized to heterogeneous mixtures of convex particles [2, 7, 8], but we restrict our attention to mixtures of circular disks [1]. We will simply quote the results we need, and refer to the literature for details on the derivations [1, 9–12].

We start with the canonical partition function for a collection of hard disks with radii R_j and copy numbers n_j, enclosed in an area A. We neglect boundary effects, and also omit contributions from velocities and internal degrees of freedom, to concentrate on the configurational entropy only. The remaining configurational partition function depends on the many-particle interaction energy, $U(\{\vec{x}\})$,

$$Z(\vec{n}, A, T) = \frac{1}{\prod_j n_j!} \int d^n\vec{x}\; e^{-\beta U(\{\vec{x}\})}, \tag{S5}$$

where $\beta = 1/k_BT$ is the inverse temperature, j is the disk species index, and we use vector notation $\vec{n} = (n_1, n_2, \ldots)$ to denote the copy number distribution, with $n = \sum_j n_j$ being the total number of disks. We next factor Z by multiplying and dividing by A^n, and write

$$Z(\vec{n}, A, T) = Q(\vec{n}, A, T) \prod_j \frac{A^{n_j}}{n_j!}, \tag{S6}$$

where $Q = \frac{1}{A^n} \int d^n\vec{x}\; e^{-\beta U(\{\vec{x}\})}$ is the configuration sum. The configuration sum describes the deviation from ideal gas behavior due to the interaction energy U, which we take to be simple hard-disk repulsion. (By construction, $Q = 1$ for an ideal gas, where $U = 0$ for all configurations.)

For the computations in the next section, we will break down configurational changes as removals and insertions of particles of different sizes, and also consider area changes as a result of changed particle size. We will therefore need the chemical potential and surface tension of the disk mixture that is our protein model.

Scaled particle theory offers a simple equation of state that relates the surface tension (2D analog of negative pressure) exerted by the disks to the area footprint, number density, and size variation of the disks. Rewriting for example Eq. (6.7) of ref. [1] in our notation, we get

$$\frac{\sigma_{\text{SPT}}}{k_BT} = -\left.\frac{\partial \ln Z}{\partial A}\right|_{T,\vec{n}} = -\frac{c_A}{1 - c_A\pi\langle R^2\rangle} - \frac{\pi(c_A\langle R\rangle)^2}{(1 - c_A\pi\langle R^2\rangle)^2}. \tag{S7}$$

(Note that we use the sign convention σdA for surface tension-area work, which is the opposite sign compared to the pressure-volume convention $-pdV$ used in the original derivations of scaled particle theory). After substituting $c_A = n/A$, this expression can be brought to the more compact form

$$\frac{\sigma_{\text{SPT}}}{k_BT} = -n\frac{A - n\pi\text{Var}[R]}{\big(A - n\pi\langle R^2\rangle\big)^2}, \tag{S8}$$

where $\text{Var}[R] = \langle R^2\rangle - \langle R\rangle^2$ is the disk radius variance. Note how the size variability decreases the (negative) pressure through the variance term.

This can again be rewritten in terms of concentration, area fraction, and relative size variability by combining the concentration $c_A = n/A$ and the area fraction relation $A - n\pi\langle R^2\rangle = (1 - \phi)A$, and then the relation $\frac{n\pi\text{Var}[R]}{A} = c_A\pi\langle R^2\rangle\eta^2 = \phi\eta^2$, resulting in

$$\frac{\sigma_{\text{SPT}}}{k_BT} = -\frac{c_A}{(1-\phi)^2}\Big(1 - \frac{n\pi\text{Var}[R]}{A}\Big) = -\frac{c_A(1 - \phi\eta^2)}{(1-\phi)^2}. \tag{S9}$$

When we consider area changes in the next section, the area integral of the surface tension at constant particle numbers will also come in handy, and we therefore integrate Eq. (S8), and obtain

$$\int \frac{\sigma_{\text{SPT}}}{k_BT} dA = -n\ln\big(A - n\pi\langle R^2\rangle\big) + \frac{n^2\pi\langle R\rangle^2}{A - n\pi\langle R^2\rangle}. \tag{S10}$$

Finally, we will need the chemical potential. This is commonly divided into an ideal gas part plus a correction, called the excess chemical potential. Using $\vec{n} + \hat{e}_j$ to denote the state with an added particle of species j, the excess chemical potential is defined as the ratio

$$\frac{\Delta\mu_j}{k_BT} = -\ln\frac{Q(\vec{n} + \hat{e}_j, T, A)}{Q(\vec{n}, T, A)}. \tag{S11}$$

Using manipulations similar to those that lead to Eqs. (S7) and (S8), the scaled-particle theory approximation given by, e.g., refs. [1, 9], can be rewritten in the form

$$\frac{\Delta\mu_j}{k_BT} = -\ln\Big(1 - \frac{n\pi\langle R^2\rangle}{A}\Big) + \frac{n(\pi R_j^2 + 2\pi R_j\langle R\rangle)}{A - n\pi\langle R^2\rangle} + \left(\frac{n\pi R_j\langle R\rangle}{A - n\pi\langle R^2\rangle}\right)^2, \tag{S12}$$

where the averages should be computed with copy numbers $\vec{n}$, i.e., without the test particle present.

From the definition of $\Delta\mu$ (Eq. (S11)), one can see that $e^{-\beta\Delta\mu} = \frac{Q(\vec{n}+\hat{e}_j,T,A)}{Q(\vec{n},T,A)}$ also has a probabilistic interpretation, namely as the probability that a test particle can

be inserted somewhere in the fluid without overlapping with the other particles. This observation, which is exact, is in fact the starting point for one way to derive scale-particle theory (see e.g., [1, 9]), by using a clever approximation to account for the overlapping exclusion zones in Fig. 1 of the main paper.

Finally, the total chemical potential is given by the ratio of partition functions,

$$\frac{\mu_j}{k_BT} = -\ln\frac{Z(\vec{n}+\hat{e}_j,T,A)}{Z(\vec{n},T,A)}. \tag{S13}$$

If we substitute Eq. (S6) and then Eq. (S12), we get the scaled-particle approximation to the total chemical potential, namely,

$$\begin{aligned}\frac{\mu_j}{k_BT} &= -\ln\frac{A^{n_j+1}}{(n_j+1)!}\frac{n_j!}{A^{n_j}} + \Delta\mu_j \qquad\qquad (S14)\\ &= -\ln\Big(\frac{A-n\pi\langle R^2\rangle}{n_j+1}\Big)\\ &\quad + \frac{n(\pi R_j^2+2\pi R_j\langle R\rangle)}{A-n\pi\langle R^2\rangle} + \left(\frac{n\pi R_j\langle R\rangle}{A-n\pi\langle R^2\rangle}\right)^2. \qquad (S15)\end{aligned}$$

III. ENTROPY CHANGE UNDER A GATING TRANSITION

We now derive our main results. Specifically, we will consider a situation with a single channel crowded by other proteins that do not change their configuration. We denote the copy number vector and total number of the crowders by $\vec{N}$ and N respectively, which contains no channels in any state. The state with a channel in state i ($i = o, c$ for the open and closed state respectively) will then have the copy number vector $\vec{N}+\hat{e}_i$.

In the main text, we use G to denote a generic free energy. Here, we will be more precise, and use F and G for the free energy in the constant area and constant tension ensembles respectively. In the thermodynamic limit, they are related by a Legendre transformation $G(\vec{n},\sigma,T) = F(\vec{n},A,T) - \sigma A$, where σ is the surface tension.

A. Small expansion parameter

When computing the gating energy changes, we expand in various small parameters. Specifically, we will consider the total area, or total lipid area, to be much larger than the area of a single protein of any species, but comparable to the total crowder footprint $N\pi\langle R^2\rangle$. This means that $\pi R_j^2/A$ is a small parameter for all protein radii R_j, but $N\pi R_j^2/A$ ($=\phi$) is not small. In a typical *E. coli* cell, $A = 5\ \mu\text{m}^2$, which means that $\pi R_j^2/A \sim 10^{-5}$ (for $R_o = 3$ nm). We will neglect such small terms.

B. Results for the constant area ensemble

To compute the free energy changes of a conformational change at constant total area, e.g., changing a particle from species i (say, a closed channel) to species j (say, an open channel), we subdivide the reaction into one insertion and one removal, by multiplying and dividing by the partition function of the intermediate state,

$$\begin{aligned}\frac{\Delta F_{i\to j}}{k_BT} &= -\ln\frac{Z(\vec{N}+\hat{e}_j,A,T)}{Z(\vec{N}+\hat{e}_i,A,T)} \qquad (S16)\\ &= -\ln\Big(\frac{Z(\vec{N}+\hat{e}_j,A,T)}{Z(\vec{N},A,T)}\frac{Z(\vec{N},A,T)}{Z(\vec{N}+\hat{e}_i,A,T)}\Big). \qquad (S17)\end{aligned}$$

Splitting the product of ratios, we can compare with Eq. (S14) to identify the free energy change as the difference of chemical potentials for the two configurations,

$$\frac{\Delta F_{i\to j}}{k_BT} = \underbrace{-\ln\frac{Z(\vec{N}+\hat{e}_j,A,T)}{Z(\vec{N},A,T)}}_{\mu_j(\vec{N},A,T)/k_BT} \underbrace{+\ln\frac{Z(\vec{N}+\hat{e}_i,A,T)}{Z(\vec{N}+\hat{e}_i,A,T)}}_{-\mu_i(\vec{N},A,T)/k_BT}. \tag{S18}$$

This means that we can use Eq. (S14) with $j = o, c$ to compute the entropic contribution to the free energy change. Using R_p to denote crowder radii, we get

$$\begin{aligned}\frac{\Delta F}{k_BT} &= \frac{\mu_o(\vec{N},A,T)-\mu_c(\vec{N},A,T)}{k_BT} \qquad (S19)\\ &= \frac{N\pi(R_o^2-R_c^2)+2N\pi\langle R_p\rangle(R_o-R_c)}{A-N\pi\langle R_p^2\rangle}\\ &\quad + \frac{N\pi\langle R_p\rangle^2\times N\pi(R_o^2-R_c^2)}{(A-N\pi\langle R_p^2\rangle)^2}. \qquad (S20)\end{aligned}$$

To simplify, we first identify changes in area $\Delta A = \pi(R_o^2-R_c^2)$, and circumference $\Delta C = 2\pi(R_o-R_c)$,

$$\frac{\Delta F}{k_BT} = \frac{N\langle R_p\rangle\Delta C}{A-N\pi\langle R_p^2\rangle} + \frac{N\Delta A}{A-N\pi\langle R_p^2\rangle}\left(1+\frac{N\pi\langle R_p\rangle^2}{A-N\pi\langle R_p^2\rangle}\right). \tag{S21}$$

Next, we use the same simplifications that lead to Eq. (S9), and end up with

$$\frac{\Delta F}{k_BT} = \frac{c_A\langle R_p\rangle}{1-\phi}\Delta C + \frac{c_A(1-\phi\eta^2)}{(1-\phi)^2}\Delta A. \tag{S22}$$

The coefficients of ΔC and ΔA are the line and surface tensions tabulated on line three of table I in the main text. The negative surface tension of the crowders (Eq. (S9)) acts to oppose an increased radius of the protein, because increasing the protein footprint decreases the area available to the rest of crowders. The quantities in these coefficients should be computed without the channel present (although computing them with the channel present would only make a small difference). The

properties of the channel itself only enter through ΔC and ΔA.

We can obtain the uniform crowders result (line 2 of main text table I) as a special case, by replacing the mean radius by a single value, $\langle R_p\rangle \to R_p$, and set the coefficient of variation, η^2, to zero.

Next, we consider the constant tension ensemble, and show that we recover only the line tension effect, i.e., the ΔC term, in that case.

C. The constant tension ensemble

For the constant tension ensemble, the statistical mechanics recipe is to introduce an external tension σ, i.e., an external loading device with energy $-\sigma A$. We also include a term H_{lipids} for lipid elastic energy as a function of area, and integrate over all areas,

$$\Xi(\vec{n},\sigma,T) = \int dA e^{\beta(\sigma A - H_{\text{lipids}})} Z(\vec{n},A,T). \tag{S23}$$

In Sec. V, we show that real membranes are too stiff for lipid elasticity to give significant contributions to the gating energy of a single channel. This means that the above integral will be dominated by the area $A_{\vec{n}} = A_0 + n\pi\langle R^2\rangle$, where A_0 is the total unstretched lipid area. To good approximation, we can therefore set $e^{-\beta H_{\text{lipids}}} \approx \delta(A - A_{\vec{n}})$, and think of the lipids as having constant area and infinite stiffness. This makes it easy to evaluate the area integral,

$$\Xi(\vec{n},\sigma,T) \approx Z(\vec{n},A_{\vec{n}},T)e^{\beta\sigma A_{\vec{n}}}, \tag{S24}$$

and we recover the free energy of the constant tension ensemble as the Legendre transformation of the free energy for the constant area ensemble,

$$\underbrace{-k_BT\ln\Xi(\vec{n},\sigma,T)}_{G(\vec{n},\sigma,T)} \approx \underbrace{-k_BT\ln Z(\vec{n},A_{\vec{n}},T) - \sigma A_{\vec{n}}}_{F(\vec{n},A_{\vec{n}},T)-\sigma A_{\vec{n}}}. \tag{S25}$$

D. Results for the constant tension ensemble

We now return to our test problem, and denote the crowder copy numbers by $\vec{N}$, the presence of a channel in state $i = o, c$ by $\vec{N} + \hat{e}_i$ etc. We can then divide the total free energy change into three contributions: removal of a closed channel at area $A_{\vec{N}+\hat{e}_c}$, an overall area change $A_{\vec{N}+\hat{e}_c} \to A_{\vec{N}+\hat{e}_o} = A_{\vec{N}+\hat{e}_c} + \Delta A$ with no channel present, and insertion of an open channel at area $A_{\vec{N}+\hat{e}_o}$:

$$\begin{aligned}\Delta G = &\underbrace{-\mu_c(\vec{N},A_{\vec{N}+\hat{e}_c},T)}_{\text{Removing a closed channel.}} \\ &\underbrace{-\sigma\Delta A + \int_{A_{\vec{N}+\hat{e}_c}}^{A_{\vec{N}+\hat{e}_o}} \sigma_{\text{SPT}}(\vec{N})dA}_{\text{Area change with the channel absent.}} \\ &+ \underbrace{\mu_o(\vec{N},A_{\vec{N}+\hat{e}_o},T)}_{\text{Inserting an open channel.}}\quad .\end{aligned} \tag{S26}$$

Substituting Eq. (S10) and Eq. (S15), and assuming that the crowder background does not contain any other channels ($N_o = N_c = 0$), we get (after collecting terms)

$$\begin{aligned}\frac{\Delta G}{k_BT} = &-\ln\left(A_0+\pi R_o^2\right) + \ln\left(A_0+\pi R_c^2\right) - \frac{\sigma\Delta A}{k_BT} \\ &+ \frac{N\pi(R_o^2 + 2\langle R_p\rangle R_o)}{A_0+\pi R_o^2} - \frac{N\pi(R_c^2+2\langle R_p\rangle R_c)}{A_0+\pi R_c^2} \\ &+ \left(\frac{N\pi\langle R_p\rangle R_o}{A_0+\pi R_o^2}\right)^2 - \left(\frac{N\pi\langle R_p\rangle R_c}{A_0+\pi R_c^2}\right)^2 - N\ln\left(\frac{A_0+\pi R_o^2}{A_0+\pi R_c^2}\right) \\ &+ \frac{N^2\pi^2\langle R_p\rangle^2(R_o^2-R_c^2)}{A_0^2\left(1+\pi R_o^2/A_0\right)\left(1+\pi R_c^2/A_0\right)}.\end{aligned} \tag{S27}$$

Next, we Taylor expand in the small parameters $\pi R_{o,c}/A_0$, collect coefficients of ΔC and ΔA (most of which cancel), and end up with the following lowest order result:

$$\frac{\Delta G}{k_BT} = \frac{N\langle R_p\rangle\Delta C}{A_0} - \frac{\sigma\Delta A}{k_BT} + \text{small terms}, \tag{S28}$$

Noting that $N/A_0 = c_A/(1-\phi)$ and discarding the small terms, we finally get

$$\frac{\Delta G}{k_BT} = \frac{c_A\langle R_p\rangle\Delta C}{1-\phi} - \frac{\sigma\Delta A}{k_BT}. \tag{S29}$$

Comparing with the constant area result of Eq. (S22), we see that the contribution from the crowding surface tension has cancelled, but that the coefficient of ΔC is the same, namely the line tension in table I of the main text. The extra term $-\frac{\sigma\Delta A}{k_BT}$ reflects the work done by the loading device during the area change, and is independent of crowding conditions.

IV. ACCOUNTING FOR DEFORMATION ZONES AROUND THE PROTEINS

As noted in the main text, we have so far neglected protein-protein interactions mediated by elastic deformations of the lipids in the vicinity of proteins, which can arise for example from a height mismatch of the protein hydrophobic core and the lipid equilibrium thickness [13]. Such interactions can give rise to rich and interesting many body effects [14], and are outside the scope of this paper.

However, we can make a phenomenological statement about one simple example, namely the case where one state of the channel (the open state, say) deforms its surrounding membrane in a way that repels other proteins, while the thickness of the other state, and all crowders, match the membrane equilibrium thickness, so that they do not interact via membrane deformations. In this case, we can account for the effect by assigning a slightly larger radius to that state, say, $\tilde{R}_o = R_o + \lambda$, where λ characterizes the size of the deformation region around the protein. The interesting result that comes out is that the surface tension terms no longer cancel in the constant tension ensemble, and hence the crowding effect could be substantially larger than our previous results. The rest of this section describes this calculation.

First, we note that in the constant area ensemble, our previous calculations can be carried through exactly as above if we just substitute $R_o \to \tilde{R}_o$ everywhere. This increases the numbers, but does not lead to a qualitative change.

For the constant tension ensemble however, simple substitution does not lead to correct results. The reason is that we should use the radius $\tilde{R}_o$ (the radius seen by other disks) when we compute the excess chemical potentials, but stick with R_o (the radius seen by the lipids) when we compute the change in total area. This means that the lowest order ΔA terms do not cancel, and we are left with some new terms. Specifically, if we break up the contributions in the same way as in Eq. (S26), we get

$$\begin{aligned}\Delta G = & \underbrace{-\mu_c(\vec{N}, A_{\vec{N}+\hat{e}_c}, T)}_{\text{Removing disk with radius } R_c.} \\ & \underbrace{-\sigma\Delta A + \int_{A_{\vec{N}+\pi R_c^2}}^{A_{\vec{N}+\pi R_o^2}} \sigma_{\mathrm{SPT}}(\vec{N}) dA}_{\text{Area change from conformational change.}} \\ & + \underbrace{\mu_{\tilde{o}}(\vec{N}, A_{\vec{N}+\hat{e}_o}, T)}_{\text{Inserting disk with effective radius } \tilde{R}_o.} . \end{aligned} \tag{S30}$$

Substituting the appropriate expressions from Eq. (S10) and Eq. (S15) and collecting terms, we get

$$\begin{aligned}\frac{\Delta\tilde{G}}{k_BT} = & + \ln\Big(\frac{A_0+\pi R_c^2}{A_{\vec{N}+\hat{e}_c}}\Big) - \frac{N\pi(R_c^2+2\langle R_p\rangle R_c)}{A_0+\pi R_c^2} - \Big(\frac{N\pi\langle R_p\rangle R_c}{A_0+\pi R_c^2}\Big)^2 \\ & - N\ln\Big(\frac{A_0+\pi R_o^2}{A_0+\pi R_c^2}\Big) + \frac{N^2\pi^2\langle R_p\rangle^2(R_o^2-R_c^2)}{A_0^2\big(1+\pi R_o^2/A_0\big)\big(1+\pi R_c^2/A_0\big)} - \frac{\sigma\Delta A}{k_BT} \\ & - \ln\Big(\frac{A_0+\pi\tilde{R}_o^2}{A_{\vec{N}+\hat{e}_o}}\Big) + \frac{N\pi(\tilde{R}_o^2+2\langle R_p\rangle\tilde{R}_o)}{A_0+\pi R_o^2} + \Big(\frac{N\pi\langle R_p\rangle\tilde{R}_o}{A_0+\pi R_o^2}\Big)^2. \end{aligned} \tag{S31}$$

If we again Taylor expand in the small parameter $\pi R_j^2/A_0$, we get less cancellations than in Eq. (S27), namely,

$$\begin{aligned}\frac{\Delta\tilde{G}}{k_BT} = & \frac{2\pi\langle R_p\rangle(\tilde{R}_o - R_c)}{A_0} - \frac{\sigma\Delta A}{k_BT} \\ & + \frac{N}{A_0}\pi(\tilde{R}_o^2 - R_o^2)\Big(1 + \frac{N\pi\langle R_p\rangle^2}{A_0}\Big) + \text{small terms}. \end{aligned} \tag{S32}$$

After discarding the small terms, and further simplifications where we again trade area and copy numbers for concentrations and area fractions, we finally get

$$\frac{\Delta\tilde{G}}{k_BT} \approx \frac{c_A\langle R_p\rangle\Delta\tilde{C}}{1-\phi} - \frac{\sigma\Delta A}{k_BT} + \frac{c_A(1-\phi\eta^2)}{(1-\phi)^2}\pi(\tilde{R}_o^2 - R_o^2), \tag{S33}$$

where $\Delta\tilde{C} = 2\pi(\tilde{R}_o - R_c)$ is the change in channel circumference experienced by the other proteins, and the extra last term can be identified as minus the entropic surface tension of Eq. (S9) times the area of the deformation zone. The interpretation is that the deformation zones induces a decrease of the available area for the crowders, which in turn induces a surface-tension contribution to the crowding effect.

With a realistic value of $\lambda = 1$ nm [13], and our numerical test parameters ($\phi = 0.5$ protein area fraction, crowder size $\langle R_p\rangle = R_p = 1$ nm, $c_A = 0.16$ proteins/nm^2, $\eta^2 = 0$, and a size change from $R_c = 2$ nm to $R_o = 3$ nm), we get

$$\frac{c_A\langle R_p\rangle\Delta\tilde{C}}{1-\phi} = 4k_BT, \quad \frac{c_A\pi(\tilde{R}_o^2 - R_o^2)}{(1-\phi)^2} = 14k_BT, \tag{S34}$$

i.e., $\Delta\tilde{G}_{\mathrm{crowd}} = 18k_BT$ instead of just $1k_BT$ with $\lambda = 0$, a very significant increase.

V. NEGLECTING LIPID ELASTICITY

When approximating the constant tension ensemble with a constant lipid area, we assumed that the strain in the lipids does not change significantly upon gating. We also neglected thermal fluctuations in lipid area. Sim-

ilarly, we neglected the elastic energy of lipids in the constant area ensemble.

In this section, we will motivate these assumptions by using a simple model of lipid elasticity to argue that accounting for these effects only gives rise to small corrections, so that neglecting elastic deformations of the lipids is a legitimate approximation.

We will use the harmonic model for a membrane patch with area A and unstretched lipid area A_0,

$$H_{\text{lipids}} = \frac{\kappa_A}{2} A_0 \left(\frac{A - n\pi\langle R^2\rangle - A_0}{A_0} \right)^2 = \frac{\kappa_A}{2A_0}(A - A_{\vec{n}})^2, \tag{S35}$$

where we used the definition $A_{\vec{n}} = A_0 + n\pi\langle R^2\rangle$ in the last equality. Many lipid bilayers have an area compression modulus κ_A around 0.25 J/m^2 $\sim 60 k_B T$/nm^2 (after correction for bending fluctuations), with cholesterol-rich and biological membranes being even stiffer [15].

A. Neglecting lipid elasticity in the constant area ensemble

If we assume no prestretching of the lipid bilayer, so that $(A - A_{\vec{n}}) \sim \Delta A$, then the change in lipid elastic energy (Eq. (S35)) is of the order $\Delta H_{\text{lipids}} \sim \kappa_A \Delta A^2 / 2A_0$. With our numerical test parameters ($A_0 = A(1-\phi) = A/2$, $\Delta A = 5\pi$ nm^2, $\kappa_A \approx 60 k_B T$/nm^2), and a patch area on the order 1 μm^2, this gives $\Delta H_{\text{lipids}} \sim 0.02 k_B T$, which can be safely neglected.

B. Constant lipid area in the constant tension ensemble

To motivate the approximation of Eq. (S24), constant lipid area in the constant tension ensemble, we use the simple lipid elastic model to estimate the contributions from lipid elasticity to the gating energy. We start with some numerical estimates.

Typical MscL gating tensions are $\sigma_0 \sim 0.3 - 1.3\ k_B T$/nm^2, which gives rise to a lipid strain of $\frac{\sigma_0}{\kappa_A} \approx 0.005 - 0.02$. The crowding surface tension with our numerical test parameters ($\phi = 0.5$ protein area fraction, $R_p = 1$ nm, $c_A = 0.16$ proteins/nm^2, and $\eta^2 = 0$), is $-\sigma_{\text{SPT}} = k_B T c_A/(1-\phi)^2 = 0.64\ k_B T$/nm^2, which induces a strain of magnitude 10^{-2}, comparable the gating strain.

The crowding tension changes with total area, in a way that can be characterized by an entropic compression modulus,

$$\kappa_{\text{SPT}} = -A_0 k_B T \frac{\partial^2 \ln Z}{\partial A^2} = A_0 \frac{\partial \sigma_{\text{SPT}}}{\partial A}. \tag{S36}$$

Differentiating Eq. (S8), we get

$$\kappa_{\text{SPT}} = \frac{n A_0 k_B T}{\left(A - n\pi\langle R^2\rangle\right)^2} + \frac{2A_0 k_B T n^2 \pi \langle R\rangle^2}{\left(A - n\pi\langle R^2\rangle\right)^3}. \tag{S37}$$

In this expression, A_0 is truly a constant (by definition of the compression modulus), but since we expect the lipid strain to be small, we can get a numerical estimate by using $A_0 \approx A - n\pi\langle R^2\rangle = A(1-\phi)$, which allows us to simplify in the usual way, and write

$$\kappa_{\text{SPT}} \approx \frac{c_A k_B T}{(1-\phi)} \Big(1 + \frac{c_A 2\pi \langle R\rangle^2}{1-\phi} \Big). \tag{S38}$$

With our numerical test parameters and $\kappa_A = 60\ k_B T$/nm^2, we get $\kappa_{\text{SPT}}/\kappa_A \approx 0.016$, so the entropic compression modulus is insignificant compared to the lipid stiffness.

In light of the above tension estimates, an estimated upper bound on the lipid strain near MscL gating conditions is therefore

$$\frac{\sigma_0 - \sigma_{\text{SPT}}}{\kappa_A + \kappa_{\text{SPT}}} \lesssim \frac{2\sigma_0}{\kappa_A} \sim 0.03. \tag{S39}$$

This is not quite as small as $\pi R^2/A$, but still small enough that we can safely neglect terms of that magnitude.

Next, we assess the importance of lipid area changes and fluctuations by computing the partition function Ξ using a saddle-point approximation, i.e., expand fluctuations to second order, and show that we recover the results based on Eq. (S24), plus small correction terms.

The above estimates strongly suggest that only areas close to $A_{\vec{n}}$ will contribute significantly to the constant tension partition function Ξ in Eq. (S23), and we therefore expand the canonical partition function Z to second order around that point. We get

$$\ln Z(A, \vec{n}, T) = \ln Z(A_{\vec{n}}, \vec{n}, T) + \frac{\partial \ln Z}{\partial A}\Big|_{A_{\vec{n}}} (A - A_{\vec{n}}) + \frac{1}{2} \frac{\partial^2 \ln Z}{\partial A^2}\Big|_{A_{\vec{n}}} (A - A_{\vec{n}})^2 + \ldots, \tag{S40}$$

and upon substituting Eq. (S36) and Eq. (S7), we can write this in the form

$$\ln Z(A, \vec{n}, T) \approx \ln Z(A_{\vec{n}}, \vec{n}, T) - \beta \sigma_{\text{SPT}} (A - A_{\vec{n}}) - \frac{\beta \kappa_{\text{SPT}}}{2A_0} (A - A_{\vec{n}})^2, \tag{S41}$$

where it is understood that σ_{SPT} and κ_{SPT} are evaluated at $A = A_{\vec{n}}$. Inserting the simple lipid energy and the above expansion in Eq. (S23), we get

$$\Xi(\sigma,\vec{n},T)=\int dA Z(A,\vec{n},T)\exp\left(\beta\sigma A-\frac{\beta\kappa_A}{2A_0}(A-A_{\vec{n}})^2\right) \tag{S42}$$

$$\approx Z(A_{\vec{n}},\vec{n},T)e^{\beta\sigma A_{\vec{n}}}\int dA\exp\left(\beta(\sigma-\sigma_{\rm SPT})(A-A_{\vec{n}})-\frac{\beta(\kappa_A+\kappa_{\rm SPT})}{2A_0}(A-A_{\vec{n}})^2\right). \tag{S43}$$

The function in the exponent takes a maximum at $A^*_{\vec{n}}=A_{\vec{n}}+A_0\left.\frac{\sigma-\sigma_{\rm SPT}}{\kappa_A+\kappa_{\rm SPT}}\right|_{A_{\vec{n}}}$, which is indeed very close to $A_{\vec{n}}$, since $A_0<A_{\vec{n}}$, and $\frac{\sigma-\sigma_{\rm SPT}}{\kappa_A+\kappa_{\rm SPT}}\ll 1$. We can now evaluate Ξ approximately, since Eq. (S43) is a Gaussian integral, and get the saddle point approximation

$$\Xi(\sigma,\vec{n},T)\approx Z(A_{\vec{n}},\vec{n},T)e^{\beta\sigma A_{\vec{n}}}\exp\left(\frac{\beta A_0}{2}\frac{(\sigma-\sigma_{\rm SPT})^2}{\kappa_A+\kappa_{\rm SPT}}\right)\left.\sqrt{\frac{2\pi k_BTA_0}{\kappa_A+\kappa_{\rm SPT}}}\right|_{A_{\vec{n}}}. \tag{S44}$$

After discarding irrelevant constants, we recover the free energy of Eq. (S25), with two correction terms that we denote G_1 and G_2,

$$\underbrace{G(\sigma,\vec{n},T)\approx -k_BT\ln Z(A_{\vec{n}},\vec{n},T)-\sigma A_{\vec{n}}}_{\text{Eq. (S25)}}\underbrace{-\frac{A_0}{2}\frac{(\sigma-\sigma_{\rm SPT})^2}{\kappa_A+\kappa_{\rm SPT}}}_{=G_1(A_{\vec{n}},\vec{n},T)}+\underbrace{\frac{k_BT}{2}\ln\big(1+\frac{\kappa_{\rm SPT}}{\kappa_A}\big)}_{=G_2(A_{\vec{n}},\vec{n},T)}, \tag{S45}$$

with all terms evaluated at area $A_{\vec{n}}$. What we need to show, is that the correction terms G_1 and G_2 indeed produce only small contributions to the overall gating tension.

We start with G_2. Since $\frac{\kappa_{\rm SPT}}{\kappa_A}\ll 1$, we can Taylor expand the logarithm, and obtain $G_2\approx k_BT\kappa_{\rm SPT}/2\kappa_A$. But for the same reason, we see that G_2 is already a small quantity, and therefore cannot make a significant contribution to the gating free energy.

For G_1, a little more effort is needed. We start by noting that we can ignore the entropic compression modulus, since it only contributes a factor $\frac{\kappa}{\kappa_{\rm SPT}+\kappa_A}\approx(1-\frac{\kappa_{\rm SPT}}{\kappa_A}+\ldots)$, i.e., a small correction to ΔG_1. Next, we rewrite $\sigma_{\rm SPT}$ from Eq. (S8), substitute $\mathrm{Var}(R)=\langle R^2\rangle-\langle R\rangle^2$, and use the fact that $A-n\pi R^2=A_0$ when $A=A_{\vec{n}}$. This leads to

$$\frac{\sigma_{\rm SPT}}{k_BT}=-n\frac{A_0+n\pi\langle R\rangle^2}{A_0^2}=-\frac{n}{A_0}-\Big(\frac{n}{A_0}\Big)^2\pi\langle R\rangle^2. \tag{S46}$$

We now consider the gating energy contribution, for the case of N crowders and a single channel that changes radius from R_c to R_o. Using the definition of G_1 in Eq. (S45), we get

$$\Delta G_1=-\frac{A_0}{2\kappa_A}\Big(\big(\sigma-\sigma_{\rm SPT}(\vec{N}+\hat{e}_o)\big)^2-\big(\sigma-\sigma_{\rm SPT}(\vec{N}+\hat{e}_o)\big)^2\Big), \tag{S47}$$

where we have written out the copy number distribution arguments of the tensions. This can be rewritten as

$$\Delta G_1=-\frac{A_0}{\kappa_A}\left(\sigma-\frac{\sigma_{\rm SPT}(\vec{N}+\hat{e}_o)+\sigma_{\rm SPT}(\vec{N}+\hat{e}_c)}{2}\right)\times\big(\sigma_{\rm SPT}(\vec{N}+\hat{e}_c)-\sigma_{\rm SPT}(\vec{N}+\hat{e}_o)\big). \tag{S48}$$

For order of magnitude estimates, approximating $\frac{1}{2}\big(\sigma_{\rm SPT}(\vec{N}+\hat{e}_o)+\sigma_{\rm SPT}(\vec{N}+\hat{e}_c)\big)\approx\sigma_{\rm SPT}$ (with unspecified channel conformation) is good enough. The difference in the last factor must be treated with more care. Substituting Eq. (S46) with $n=N+1$ and $\langle R\rangle=\frac{N\langle R_p\rangle+R_{o,c}}{N+1}$ for the mean protein radius in the two states ($\langle R_p\rangle$ is the mean radius of the crowders only), we get

$$\frac{\Delta G_1}{k_BT}=-A_0\frac{\sigma-\sigma_{\rm SPT}}{\kappa_A}\times\Big(\frac{N+1}{A_0}\Big)^2\Big(\frac{(N\langle R_p\rangle+R_o)^2-(N\langle R_p\rangle+R_c)^2}{(N+1)^2}\Big). \tag{S49}$$

Expanding the squares in the last factor, substituting $\frac{N}{A_0}=\frac{c_A}{1-\phi}$, and neglecting a term of order $\pi R^2/A_0$, we finally get

$$\frac{\Delta G_1}{k_BT}=-\Big(\frac{\sigma-\sigma_{\rm SPT}}{\kappa_A}\Big)\frac{c_A\langle R_p\rangle\Delta C}{1-\phi}. \tag{S50}$$

This is a negative correction to the familiar line tension term, which smaller than the lowest order term of Eq. (S29) by a factor $\frac{\sigma_0-\sigma_{\rm SPT}}{\kappa_A}\lesssim 10^{-2}$, indeed a small correction.

[1] J. L. Lebowitz, E. Helfand, and E. Praestgaard, J. Chem. Phys., **43**, 774 (1965).
[2] J. Talbot, J Chem Phys, **106**, 4696 (1997).
[3] S. Mller, M. D. Croning, and R. Apweiler, Bioinformatics, **17**, 646 (2001).
[4] S. Yun *et al*, J. Proteome Res. (2010), doi: 10.1021/pr101012s.
[5] S. Takamori *et al*, Cell, **127**, 831 (2006).
[6] H. Hahne, S. Wolff, M. Hecker, and D. Becher, Proteomics, **8**, 4123 (2008).
[7] R. Gibbons, Molecular Physics, **17**, 81 (1969).
[8] T. Boublík, Mol. Phys., **29**, 421 (1975).
[9] H.-X. Zhou, J. Phys. Chem. B, **113**, 7995 (2009).
[10] E. Helfand, H. L. Frisch, and J. L. Lebowitz, J. Chem. Phys., **34**, 1037 (1961).
[11] H. Reiss, H. L. Frisch, and J. L. Lebowitz, J. Chem. Phys., **31**, 369 (1959).
[12] M. Heying and D. S. Corti, J. Phys. Chem. B, **108**, 19756 (2004).
[13] R. Phillips, T. Ursell, P. Wiggins, and P. Sens, Nature, **459**, 379 (2009).
[14] K. Kim, J. Neu, and G. Oster, Biophys. J., **75**, 2274 (1998).
[15] D. Boal, *Mechanics of the Cell* (Cambridge University Press, 2002).